Nuclear Instruments and Methods in Physics Research B 107 (1996) 204–211

ELSEVIER

NIM B
Beam Interactions with Materials & Atoms

Phase transformation induced by swift heavy ion irradiation of pure metals

H. Dammak [1], A. Dunlop *, D. Lesueur [2]

Laboratoire des Solides Irradiés, CEA / Ecole Polytechnique, 91128 Palaiseau Cedex, France

Abstract

It is now unambiguously established that high electronic energy deposition (HEED), obtained by swift heavy ion irradiation, plays an important role in the damage processes of pure metallic targets: (i) annealing of the defects created by elastic collisions in Fe, Nb, Ni and Pt, and (ii) creation of additional defects in Co, Fe, Ti and Zr. For Ti, we have recently evidenced by transmission electron microscopy observations that the damage creation by HEED is very important and leads to a phase transformation. Titanium evolves from the equilibrium hcp alpha-phase to the high pressure omega-phase. We studied the influence of three parameters on this phase transformation: ion fluence, electronic stopping power and irradiation temperature. The study of Ti and the results concerning other metals (Fe, Zr, etc.) and the semi-metal Bi allow us to propose criteria to predict in which metals HEED could induce damage: those which undergo a phase transformation under high pressure. As a matter of fact, beryllium is strongly damaged when submitted to HEED and seems to behave very similarly to titanium. The fact that such phase changes from a crystalline form to another form were only observed in those metals in which high pressure phases exist in the pressure–temperature diagram, strongly supports the Coulomb explosion model in which the generation of (i) a shock wave and (ii) collective atomic movements are invoked to account for the observed damage creation.

1. Introduction

When a high energy ion (10 MeV/nucleon) slows down in matter, it mainly loses its energy to the electronic system of the target. The electronic stopping power $S_e = -(dE/dx)_e$ dominates the nuclear stopping power (S_n) by a factor of about 1000. Strong ionization of the target atoms located along the ion trajectory occurs and highly excited electrons are ejected. The damage effect of such high electronic energy deposition (HEED) on pure metals has been studied extensively during the latter years. In particular, HEED leads to the creation of additional defects in pure metals: Fe, Zr and Ti [1,2], and in the semi-metal Bi [3].

We have recently evidenced by X-ray diffraction and transmission electron microscopy (TEM) a phase transformation in titanium after GeV uranium irradiation at low temperature (20 K) and at fluences of about 10^{13} cm^{-2} [4]. During this transformation, titanium evolves from the equilibrium hcp α-phase to the high pressure hexagonal ω-phase. A *crystalline phase transformation* has been observed for the first time as a result of the slowing-down of swift heavy ions in a pure metal. In order to determine some characteristics of the transformation we studied the influence of parameters such as the ion fluence Φ, the electronic stopping power S_e, and the irradiation temperature.

2. Phase transformation in Ti: its characteristics and mechanism

2.1. Experimental results

2.1.1. Transmission electron microscopy

A few μm thick titanium ribbons were irradiated under different conditions by GeV ions (O to U). After irradiation, the targets were electrochemically thinned [4] and then observed at 300 K using a Philips electron microscope operating at 300 keV. In Fig. 1, the experimental conditions (S_e, Φ) for three different irradiation temperatures (20, 80 and 300 K) are reported. After TEM examination, the S_e–Φ diagram could be divided into different regions.

* Corresponding author. Tel. +33 1 6933 4494, fax +33 1 6933 3022.

[1] Present address: Laboratoire CPS, Ecole Centrale Paris, grande voie des vignes, 92295 Chatenay-Malabry, France.

[2] Present address: DRECAM, Centre d'Etudes de Saclay, 91191 Gif-sur-Yvette, France.

SSDI 0168-583X(95)01032-7

(a) After low temperature irradiation (up to 80 K).

In region A ($S_e \leq 26$ keV/nm), the produced defects have no visible contrast in bright field images.

In region C ($S_e \geq 33$ keV/nm), one incoming ion produces an alignment of small objects located in the close vicinity of the projectile path (sub-region C′). The 5 nm size objects present black and white contrasts resembling those observed for dislocation loops [5]. After irradiation at high fluence (sub-region C″) the overlap of these ''tracks'' leads to a local phase transformation: for example, after irradiation at a fluence of about 10^{13} cm^{-2}, the 1 μm size alpha-matrix is almost totally transformed into 100 Å size omega ''precipitates''. The crystallographic orientation of the ''precipitates'' obeys the orientational relationship (OR) $\boldsymbol{a}_\omega \| \boldsymbol{c}_\alpha$, and $\boldsymbol{c}_\omega$ is parallel to one of the three equivalent $\boldsymbol{a}_\alpha$ directions in the alpha-matrix which can lead to the formation of one, two or three omega-variants.

Between regions A and C ($S_e \sim 30$ keV/nm), ''tracks'' are also produced (sub-region B′), but their spatial overlap induces a partial recovery of the damage in such a way that the observed ''track'' density is much smaller than the impinging ion fluence (sub-region B″).

(b) Consider now the influence of the irradiation temperature. We will compare two electrochemically thinned samples that were irradiated respectively at 80 and 300 K by 0.87 GeV lead ions (36 keV/nm) at a high fluence of about 10^{13} cm^{-2}. Fig. 2 shows images of the samples observed at room temperature by optical microscopy. One can observe the *spectacular warping* induced in the first sample ($T_{irr} = 80$ K); this results from $\alpha \rightarrow \omega$ phase transformation, as there is a significant difference between the densities of the two phases ($\Delta V(\alpha \rightarrow \omega)/V \approx -1\%$). In the second ($T_{irr} = 300$ K), TEM shows a dense dislocation structure due to the overlap of ''tracks''. Observations of samples irradiated at room temperature in region C are represented by open circles in Fig. 1; ion irradiation induces tracks after low fluence and a very dense dislocation structure after high fluence irradiation.

2.1.2. Electrical resistivity

The above TEM observations should be completed by in situ measurements to prove that ''tracks'' are formed and phase transformation takes place during irradiation. From in situ low temperature electrical resistivity results (partly reported in Ref. [2]), we extract the following points.

(a) *The initial damage production rate* $\Delta\dot{\rho}_0$ ($= (d\Delta\rho/d\Phi)$ at $\Phi = 0$, where $\Delta\rho$ is the electrical resistivity increase) increases strongly with S_e (Fig. 3). The damage efficiency ξ (ratio between the measured $\Delta\dot{\rho}_0$ and the initial damage production rate if damage was only produced in elastic collisions) reaches values as high as a few tens. Fig. 3 also shows that, in region C′ (see Fig. 1), the *initial* damage production rate is not influenced by the irradiation temperature.

(b) *The damage production curve* (DPC) ($\Delta\rho$ versus Φ) progressively evolves from an almost straight line ($S_e \approx$ a few keV/nm) to a very curved line ($S_e > 10$ keV/nm), as shown in Fig. 4. A negative curvature appears at low irradiation fluences (i.e. sub-regions B′ and C′) and is followed either by rapid saturation at high fluences, characterized by a low saturation electrical resistivity increase $\Delta\rho_\infty$ (a few μΩ cm) (B″), or by linear behaviour with very high $\Delta\rho_\infty$ (a few 10 μΩ cm) (C″).

In regions A and B, DPCs could be fitted by an expression deduced, using an homogenous spatial descrip-

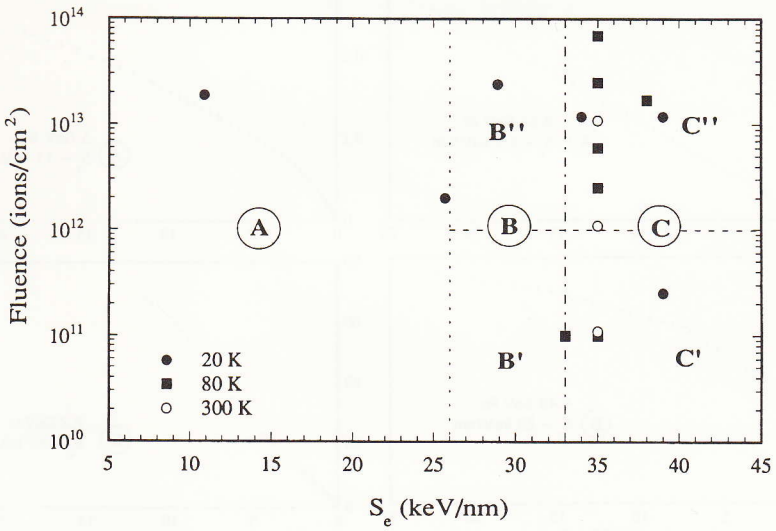

Fig. 1. Experimental parameters represented in the S_e–Φ coordinates for different irradiation temperatures. Regions A, B and C distinguish the different types of damage observed by transmission electron microscopy. Sub-regions at low fluence and high fluence are indicated by O′ and O″, respectively (see text for description).

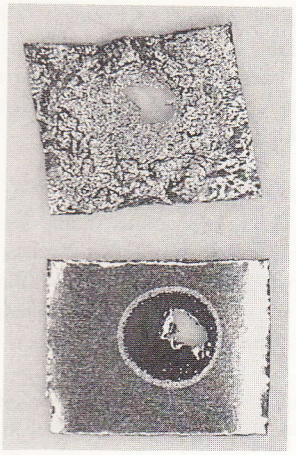

Fig. 2. Optical microscopy images of 3 mm size titanium samples electrochemically thinned at the center in order to be observed by TEM. The upper sample was irradiated at 80 K, with 45° incidence angle, by 0.87 GeV ions up to a fluence of 2×10^{13} cm^{-2}. The sample, totally transformed into the ω-phase, was subjected to strong warping due to the different densities of the α-and ω-phases of Ti. The lower sample was irradiated under the same conditions except for the irradiation temperature (300 K) and the incidence angle (0°). The sample seems to be unchanged by irradiation, but TEM observations show that it contains a very high dislocation density.

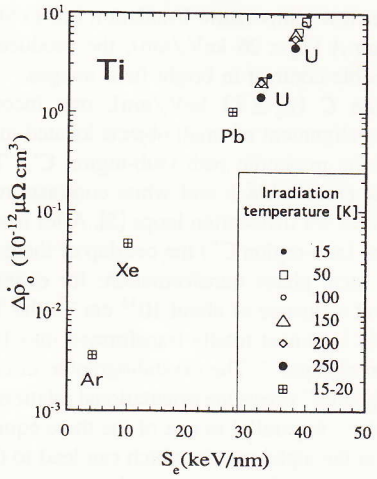

Fig. 3. Initial damage production rate for titanium versus electronic stopping power measured during irradiation at different temperatures (15–250 K) with 1–5 GeV uranium ions. The results for Ar, Xe and Pb irradiations at 15–20 K are also shown.

tion of the damage, from a phenomological model developed in a previous paper [2]. In this model, it is considered that one ion damages a cylinder of section $S_1 = \pi r_1^2$ around the ion path leading to a local resistivity increase ρ_1 inside the damaged cylinder. Some of the pre-existing defects located between two coaxial cylinders of radii r_1 and r_2 ($> r_1$, $S_2 = \pi r_2^2$) can be recombined during subsequent spatial overlap, which leads to an overall resistivity increase ρ_2 in this partly annealed matter.

In region C, at high fluence ($> 10^{12}$ cm^{-2}), small (100 Å) "precipitates" of the omega-phase are formed in the volume of the alpha-matrix, so that an inhomogeneous model has to be used to account for the resulting electrical

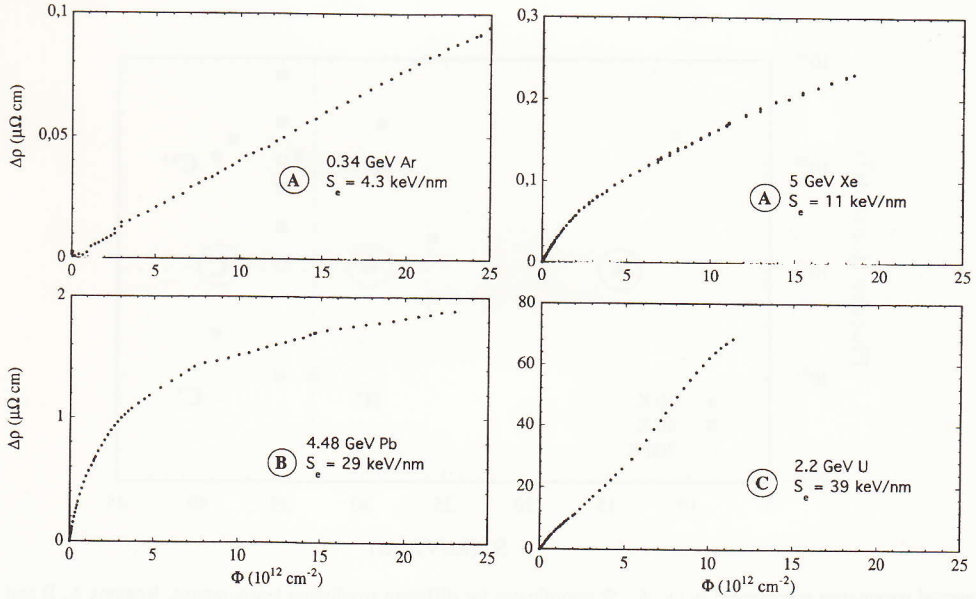

Fig. 4. Low temperature (20 K) damage production curves (electrical resistivity increase $\Delta\rho$ ($\mu\Omega$ cm) versus ion fluence Φ (10^{12} cm^{-2}) for different (Ar, Xe, Pb and U) irradiations.

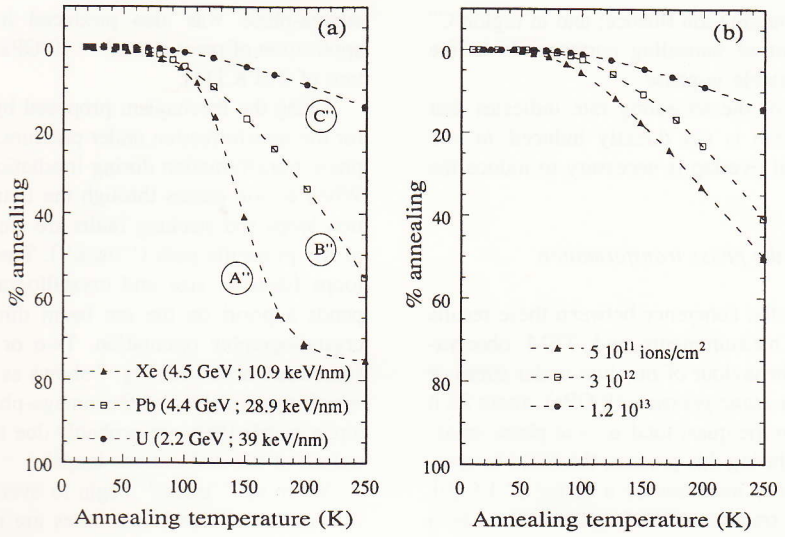

Fig. 5. Typical 10 min isochronal recovery curves for titanium irradiated at 20 K with heavy ions: (a) after irradiation at high fluence ($\sim 10^{13}$ cm^{-2}) with different ions (Xe, Pb and U); (b) after irradiation at different fluences with 2.2 GeV U ions.

resistivity. During low temperature irradiation of a Ti ribbon, in situ measurements of (i) the electrical resistance and (ii) the length of the sample allowed direct insight into the kinetics of the phase transformation [6]; both curves were fitted with an inhomogeneous model of damage creation, so that a direct determination of the density of the new phase was possible.

(c) Concerning the *damage annealing* which occurs when the irradiated sample is gradually heated to 250 K, Fig. 5 shows that:

(i) after irradiation at 20 K at the same fluence (10^{13} cm^{-2}) with various projectiles, the higher S_e, the lower the annealing percentage, and

(ii) after irradiation with the same projectile, the higher the fluence, the lower the percentage of annealing.

In accordance with TEM observations:

(i) In region A″ the extensive annealing is associated with the creation of isolated defects or small defect aggregates; in region B″ a partial annealing of the defects is associated with the fact that the number of observed tracks

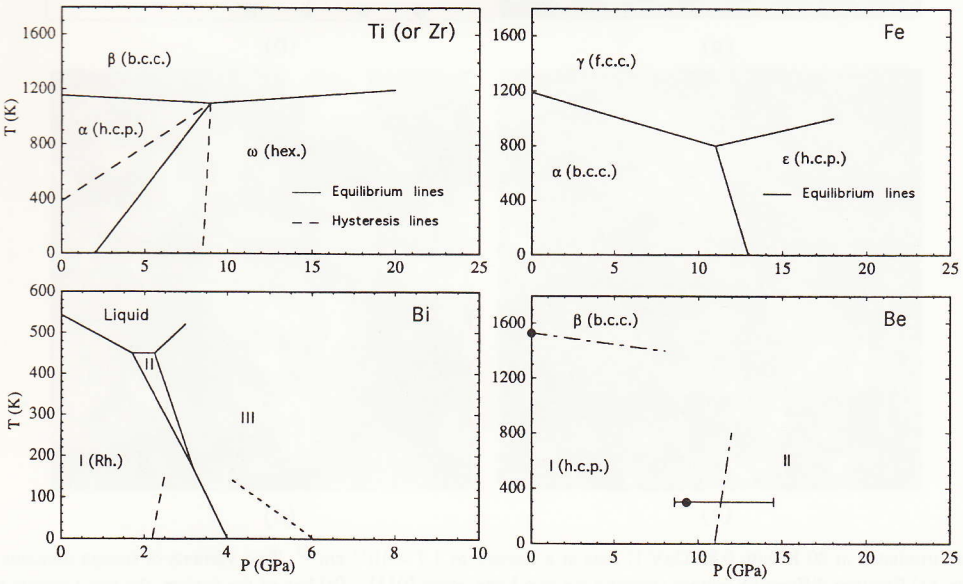

Fig. 6. Temperature–pressure phase diagrams for Ti [16], Fe [22], Bi [29,30] and Be [25–27]. The hysteresis for the transformation under pressure is very large for Ti and Zr [16], quasi-absent for Fe, wide at low temperature for Bi [30], and unknown for Be.

is smaller than the impinging ion fluence; and in region C″ the very small amount of annealing corresponds to the formation of the metastable ω-phase.

(ii) The evolution of the annealing rate indicates that the phase transformation is not directly induced *in one track*, but that a spatial overlap is necessary to induce the phase change.

2.2. A mechanism for the phase transformation

We can readily see the coherence between these results (electrical resistivity measurements and TEM observations) and the known behaviour of titanium under stress or pressure. Under a high *static pressure* (8 GPa), about 24 h are necessary to obtain the quasi-total $\alpha \rightarrow \omega$ phase transformation [7,8] in Ti; during this process, the room temperature electrical resistivity increases by a factor of 1.6 [9]. The displacive $\alpha \leftrightarrow \omega$ transformation is characterized by a wide hysteresis that allows the omega-phase to be retained in a metastable state when the pressure is removed at room temperature (Fig. 6). Moreover, when the pressure is not sufficient or is not applied for long enough, the phase transformation does not take place and only a very dense dislocation structure is observed by TEM [10]. The omega-phase was also produced in a *shock wave* by application of pressures of ~ 10 GPa at an initial temperature of 270 K [11].

Using the mechanism proposed by Rabinkin et al. [12] for the transformation under pressure, a mechanism for the phase transformation during irradiation could be proposed. When an ion passes through the titanium ribbon, dislocation loops and stacking faults are created in close vicinity of the projectile path (''track''). The distribution of these loops (density, size and crystallographic orientation) depends a priori on the ion beam direction relative to the crystallographic orientation. Two or three ω-variants are sometimes observed; Fig. 7 shows as an example a case in which two variants of the omega-phase are formed in an alpha-matrix (they are probably due to two different orientations of the dislocations loops).

When the ''tracks'' begin to overlap, i.e. when the ion fluence is increased, two cases are considered depending on the stability of the ''tracks'':

(i) The perturbation induced by a subsequent ion can lead to a partial annealing of the preexisting damage and thus to the disappearance of part of the loops that were located around the ion path (region B).

(ii) The created loops are stable and are piled up. To

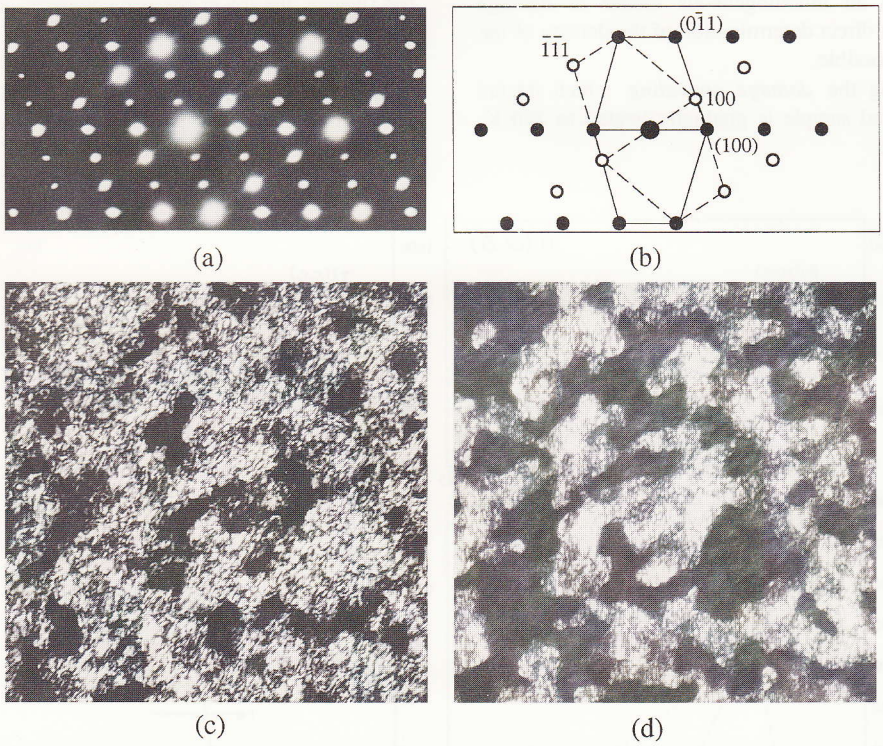

Fig. 7. Titanium irradiated at 80 K with 0.85 GeV U ions at a fluence of 1.7×10^{13} cm^{-2}. Two variants of omega domains are formed in the alpha-matrix. (a) Electron diffraction pattern showing the two Laue zones $[011]_{\omega}$; (b) key of the pattern, the two variants are represented by different spots; (c,d) dark field images obtained using two different spots of the {100} type, labelled (100) and 100 in (b). The two images are not complementary because the ω-domains are distributed in the sample volume.

minimise the stress energy, a local atomic rearrangement takes place after some incubation fluence ($\approx 10^{12}$ cm^{-2}), leading to the formation of ω-domains (region C).

3. The possibility of phase transformation in a pure metal

To explain ''track'' formation in titanium we considered the mechanisms by which the energy deposited in the electronic system is transferred to the lattice. Two models are proposed: the ''thermal spike'' (TS) and the ''Coulomb explosion'' (CE) models. In the first, the energy carried by the excited electrons returns to the lattice via efficient electron–phonon coupling, possibly leading to local melting followed by a quench [13]. In the second, the electrostatic potential energy stored in the space charge resulting from the ionization of the atoms is converted into radial kinetic energy transferred to the atoms located in the vicinity of the projectile path [14].

The similarities observed between irradiation effects and pressure effects, in particular the crystalline $\alpha \rightarrow \omega$ phase transformation in titanium, allow us to use the Coulomb explosion model to account for ''track'' formation. As a matter of fact, it has been shown, using the CE model, that collective and coherent motions of neighbouring atoms can generate a shock wave and/or low energy phonon mode excitations [14].

It is important to distinguish between the induced ion perturbation and the resulting latent damage which depends strongly on the target properties. From the CE model, the microscopic mechanical properties (damage induced by strain, pressure and shock wave) are relevant in explaining damage creation.

3.1. Zirconium

No phase transformation or ''tracks'' are observed in zirconium irradiated under similar conditions as Ti (GeV Xe to U ions, low irradiation temperature), although Zr undergoes the same phase transformation as Ti under an applied hydrostatic pressure [15,16] or when submitted to a shock wave [17]. Moreover, Ti and Zr have very similar phase diagrams (Fig. 6). On the other hand, the shape of the DPCs obtained during irradiation of Zr [2] and the absence of defects observed by TEM indicate that only region A is explored for Zr, so that the electronic stopping power above which ''tracks'' could be created is higher than for Ti.

The difference between Ti and Zr can be explained by considering the CE model. The radial recoil energy E_r transferred to the target atoms surrounding the ion path is proportional to $\eta^8/(M_2\omega_p^2)$, where η^2 is proportional to S_e for high energy ions [14], M_2 is the target atomic mass and ω_p the electron plasma frequency. Zr is about twice as heavy as Ti, so the electron energy deposition must be higher in Zr than in Ti to induce ''tracks'' or a phase transformation. Indeed, ''tracks'' are created in Zr under 18 MeV fullerene irradiation [18]; although S_e is similar to that obtained during GeV U irradiation, the density of the deposited energy is much higher using aggregate projectiles.

Hafnium, in which the $\alpha \rightarrow \omega$ phase transformation occurs at much higher pressure (about 60 GPa at 300 K) [19], can also be considered. However, to our knowledge, no irradiation experiment has been carried out on Hf, but we think that even with GeV U irradiation, the electronic energy deposition would be insufficient to create ''tracks'' or a phase transformation.

3.2. Iron

It was established in 1990 [20] that sufficiently high electronic excitations induce damage in iron. Below 40 keV/nm (region I), HEED produces a partial recovery of the defects resulting from elastic collisions. Above 40 keV/nm (region II), additional defects are created around the ion path [21]. Under these latter conditions, no microstructural defect could be seen by TEM observations at 300 K. However, the additional damage creation could be explained using the following shock-wave study results.

The P–T phase diagram of Fe [22] shows that a martensitic α(bcc) $\rightarrow$ ϵ(hcp) phase transformation occurs under a pressure of about 15 GPa at 100 K, and that in the temperature range 100–800 K the hysteresis is almost absent (Fig. 6). On the other hand, during room temperature shock-wave treatment (13 GPa) an α-iron fraction is locally transformed into the ϵ-phase, but it immediately transforms back into the α-phase as the stress is relaxed [23]. It has also been shown that microtwins are present in shock-loaded samples [24].

Considering again the irradiation effects, we think that the magnitude of the stress induced during the radial shock wave generated by the passage of the ion:

(i) is not sufficient to lead to significant lattice displacements *in region I*, i.e. to initiate the martensitic $\alpha \rightarrow \epsilon$ phase transition. But the associated vibrating lattice can induce the recombination of a portion of the interstitials and vacancies created by nuclear collisions during the irradiation; and

(ii) is sufficient to initiate a local $\alpha \rightarrow \epsilon \rightarrow \alpha$ phase change *in region II*. This double phase transformation leads to the observed additional defect creation.

3.3. Beryllium

Beryllium is a metal in which a phase transformation occurs under pressure [25,26] (Fig. 6). At room temperature and under a pressure of about 8.6–14.5 GPa, Be evolves from the hcp structure (I) to an orthorhombic structure (II) derived from (I) by a distortion of the hcp structure [26,27]. The hysteresis of the transformation is

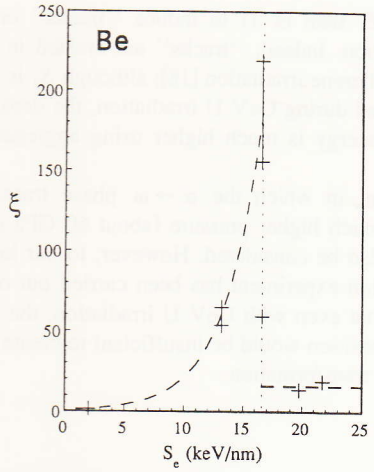

Fig. 8. Evolution of the damage creation efficiency as a function of S_e in a beryllium target irradiated at 15 K with GeV heavy ions. Note the discontinuity at $S_e = 16.5$ keV/nm.

narrow so that phase II cannot be retained at room temperature under atmospheric pressure [26]. Moreover, to our knowledge no phase diagram of Be below 300 K has been published.

The fact that Be is much lighter than Ti prompted us to test its behaviour during irradiation. The first results resemble those observed for titanium.

(i) Up to an electronic stopping power of about 16.5 keV/nm, the efficiency ξ increases strongly from 1 to ~ 100 (Fig. 8). The DPC presents an initial strong negative curvature followed by rapid saturation (Fig. 9). The DPCs could be fitted by the phenomenological model [2] described above. After irradiation at 15 K with 4.9 GeV Pb ions (13.2 keV/nm) the deduced parameters are $\rho_1/\rho_2 \approx$ 3.5, $S_2/S_1 \approx 17$ (identical to those deduced for Zr and for Ti in region A [2]) and $r_1 \approx 3$ nm.

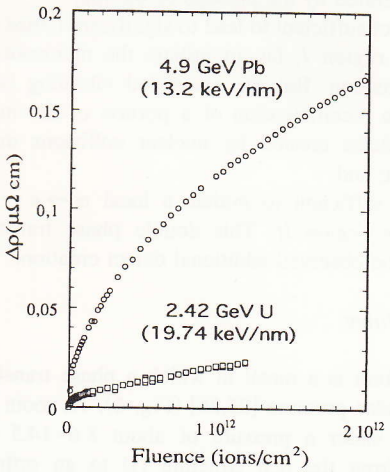

Fig. 9. Typical damage production curves registered during 15 K irradiation of beryllium with GeV Pb and U ions.

(ii) Above 16.5 keV/nm, ξ decreases to much smaller values; it is close to 20 after irradiation at 15 K with 2.42 GeV U ions (19.74 keV/nm) (Fig. 8).

(iii) Room temperature X-ray diffraction shows that all samples have the hcp structure after irradiation.

This discontinuity observed in the electrical resistivity behaviour when the electronic stopping power increases should be associated with a change in the damage process. As the I → II phase transformation occurring under static applied pressure in Be is accompanied by a 45% reduction in the electrical resistance [25], we suggest that:

(i) at low S_e, as in region A of Fig. 1 for Ti, the ion induces point defect creation, and

(ii) at high S_e, the ion can directly induce (i.e. in an individual event and not after spatial overlap as in region C of Fig. 1 for Ti) the I → II phase transformation followed eventually by the reverse transformation, similarly to what occurs for iron.

Point (ii) should be clarified by in situ low temperature X-ray diffraction in order to confirm the possibility of direct phase transformation in close vicinity of the ion path.

3.4. Bismuth

Bismuth was also studied under swift heavy ion irradiation [28]. The authors have witnessed additional damage above a S_e threshold of 24 keV/nm. In the S_e range above 30 keV/nm, irradiation induces a high saturation electrical resistivity increase. The irradiation damage is stable up to 150 K, but completely disappears after annealing up to room temperature. Using the "thermal spike" model and electrical resistivity–temperature data for thin Bi layers, the authors suggest that one ion induces an unstable amorphous "track" which subsequently crystallizes at the irradiation temperature (20 K).

The electrical resistivity results are very similar to those observed for Ti, so that an alternative interpretation, detailed below, can be put forward:

(i) The low temperature phase diagram of bismuth (Fig. 6) shows a variety of allotropic phases under high pressure [29]. Up to 5 GPa, two phase changes are observed successively, I → II → III. At low temperatures, the I ↔ III phase transformation is characterized by a hysteresis, the width of which increases when the temperature is lowered [30]. At 20 K the equilibrium pressure transformation is close to 3.5 GPa; the hysteresis width is respectively 2.2 and 4 GPa at 77 and 4.2 K.

(ii) Bismuth is a semi-metal for which electrons and holes, present at very low density (10^{-5} per atom), have an effective mass respectively 1000 and 100 times smaller than the free electron mass. Therefore, in the expression $\eta^8/(M_2\omega_p^2)$ (which is proportional to the transferred kinetic energy as discussed in Section 3.1), the high target

atomic mass is balanced by the low electron plasma frequency. Thus, radial recoil energies in the CE model for Ti and Bi are comparable.

In conclusion, during GeV U ion irradiation of Bi, the I ↔ II,III phase changes could well occur, leading, because of the large hysteresis, to high damage production (dislocations, stacking faults, etc.) and thus to a high electrical resistivity increase. Indeed, the average resistivity increment due to dislocations is 2000 times higher in Bi than in Ti or in Zr [31].

4. Conclusion

$\alpha \rightarrow \omega$ phase transformation during irradiation of titanium with swift heavy ions occurs at low temperature ($T_{irr} < \sim 80$ K), after some incubation fluence ($\sim 10^{12}$ cm^{-2}) and for electronic stopping power $S_e \geq 33$ keV/nm. The detailed study of titanium and the results for other metals (Zr, Fe and Be) and the semi-metal Bi, allow us to propose a mechanism for the damage process by swift heavy ions in metals.

The fact that damage creation was only observed in those metals for which high pressure phases exist in the pressure–temperature diagram, allows us to interpret the experimental results generally.

The phase transformations observed under pressure are usually displacive or martensitic, so that they require a shearing strain. A highly energetic ion passing through a metal generates a shock wave; the resulting stress tensor is anisotropic (when the impinging ion direction corresponds to a low symmetry crystallographic direction, for example) and a shearing stress is applied locally. The magnitude of the pressure essentially depends on the linear energy deposition, the target atomic mass and the electron plasma frequency. The response of a metal to such a stress depends on its elastic and mechanical properties. The dynamical shearing strain can lead:

(1) to stable dislocation loops or stacking faults, if the phase transformation under pressure is characterised by a wide hysteresis, or

(2) to defect creation due to the dynamic shearing strain if the hysteresis is absent.

These arguments support the Coulomb explosion model in which the generation of (i) a shock wave and (ii) collective atomic movements are invoked to account for damage creation.

References

[1] A. Dunlop and D. Lesueur, Radiat. Eff. and Def. in Solids 126 (1993) 123.
[2] H. Dammak, D. Lesueur, A. Dunlop, P. Legrand and J. Morillo, Radiat. Eff. and Def. in Solids 126 (1993) 111.
[3] E. Paumier, A. Audouard, F. Beuneu, C. Dufour, J. Dural, J.P. Girard, A. Hairie, M. Levalois, M.N. Metzner and M. Toulemonde, Radiat. Eff. and Def. in Solids 126 (1993) 181.
[4] H. Dammak, A. Barbu, A. Dunlop, D. Lesueur and N. Lorenzelli, Philos. Mag. Lett. 67 (1993) 253.
[5] J. Henry, A. Barbu, B. Leridon, D. Lesueur and A. Dunlop, Nucl. Instr. and Meth. B 67 (1992) 390.
[6] H. Dammak, thesis, CEA Report R-5668 (1994).
[7] Y.K. Vohra, E.S.K. Menon, S.K. Sikka and R. Krishnan, Acta Metall. 29 (1981) 457.
[8] A.K. Singh, Murali Mohan and C. Divakar, J. Appl. Phys. 54 (1983) 5721.
[9] V.A. Zil'Bershteyn, G.I. Nosova and E.I. Estrin, Fiz. Met. Metalloved. 35 (1973) 584.
[10] A.V. Dobromyslov, N.I. Taluts, K.M. Demchuk and A.N. Martem'ynov, Phys. Met. Metall. 65 (1988) 588.
[11] D.L. Gur'ev, L.I. Kopaneva and S.S. Batsanov, Sov. Tech. Phys. Lett. 14 (1988) 187.
[12] A. Rabinkin, M. Talianker and O. Botstein, Acta Metall. 29 (1981) 691.
[13] M. Toulemonde, E. Paumier and C. Dufour, Radiat. Eff. and Def. in Solids 126 (1993) 201.
[14] D. Lesueur and A. Dunlop, Radiat. Eff. and Def. in Solids 126 (1993) 163.
[15] M.P. Usikov and V.A. Zilbershtein, Phys. Status Solidi (a) 19 (1973) 53.
[16] S.K. Sikka, Y.K. Vohra and R. Chidambaram, Prog. Mater. Sci. 27 (1982) 245.
[17] S.G. Song and G.T. Gray III, Philos. Mag. A 71 (1995) 275.
[18] H. Dammak, A. Dunlop, D. Lesueur, A. Brunelle, S. Della-Negra and Y. Le Beyec, Phys. Rev. Lett. 74 (1995) 1135.
[19] L.C. Ming, M.H. Manghnani and K.W. Katahara, J. Appl. Phys. 52 (1981) 1332.
[20] A. Dunlop, D. Lesueur, J. Morillo, J. Dural, R. Spohr and J. Vetter, Nucl. Instr. and Meth. B 48 (1990) 419.
[21] A. Dunlop, D. Lesueur, P. Legrand and H. Dammak, Nucl. Instr. and Meth. B 90 (1994) 330.
[22] P.M. Giles, M.H. Longenbach and A.R. Marder, J. Appl. Phys. 42 (1971) 4290.
[23] L.M. Barker and R.E. Hollenbach, J. Appl. Phys. 45 (1974) 4872.
[24] J. Jacqesson, Rev. Mét. 59 (1962) 616; M. Hallouin, M. Gerland, F. Cottet, J.P. Romain and L. Matry, Société Française de Métallurgie, Journées Métallurgiques d'Automne (1986) 25.
[25] A.R. Marder, Science 142 (1963) 664.
[26] L.C. Ming and M.H. Maghnani, J. Phys. F 14 (1984) L1.
[27] V. Vijayakumar, B.K. Godwal, Y.K. Vohra, S.K. Sikka and R. Chidambaram, J. Phys. F 14 (1984) L65.
[28] C. Dufour, A. Audouard, F. Beuneu, J. Dural, J.P. Girard, A. Hairie, M. Levalois, E. Paumier and M. Toulemonde, J. Phys. Condensed Matter 5 (1993) 4573.
[29] F.P. Bundy, Phys. Rev. 110 (1958) 314.
[30] E.M. Compy, CNRS Int. Colloq. on the Physical Properties of Solids Under Pressure, Grenoble (1969) p. 453.
[31] R.A. Brown, J. Phys. F 7 (1977) L297.